

Supporting Information

Donor–Acceptor Polymers Containing Thiazole-Fused Benzothiadiazole Acceptor Units for Organic Solar Cells

Tomoya Nakamura^a, Yasuhisa Ishikura^a, Noriko Arakawa^a, Megumi Hori^a, Motoi Satou^a, Masaru Endo^a, Hisashi Masui^b, Shinichiro Fuse^c, Takashi Takahashi^b, Yasujiro Murata^a, Richard Murdey^a, and Atsushi Wakamiya^{a,*}

^aInstitute for Chemical Research, Kyoto University, Gokasho, Uji, Kyoto 611-0011, Japan

^bDepartment of Pharmaceutical Sciences, Yokohama University of Pharmacy, 601, Matano-cho, Totsuka-ku, Yokohama 245-0066, Japan

^cLaboratory for Chemistry and Life Science, Institute of Innovative Research, Tokyo Institute of Technology, 4259 Nagatsuta-cho, Midori-ku, Yokohama, Kanagawa 226-8503, Japan

Thermogravimetric Analysis

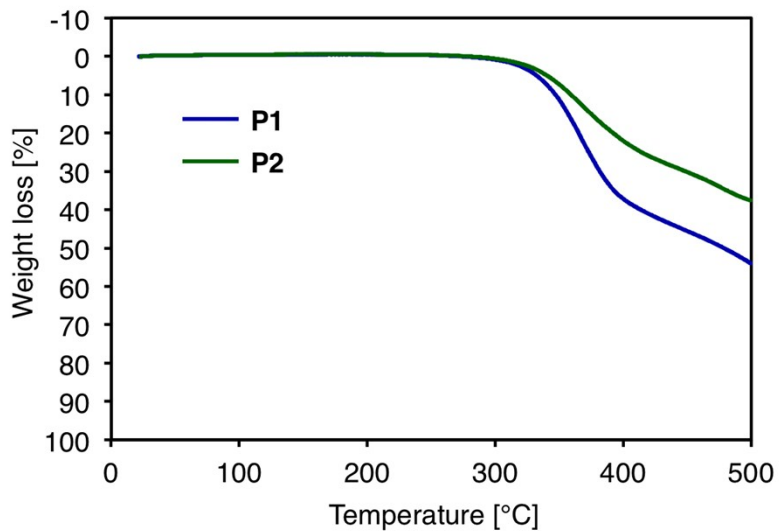


Fig. S1 Thermogravimetric analysis of D–A polymers under nitrogen atmosphere with a heating rate of $10\text{ }^{\circ}\text{C min}^{-1}$.

Tauc Plots

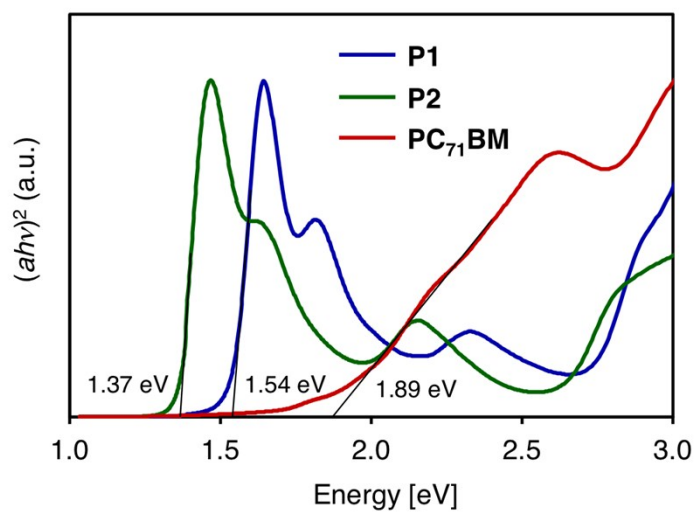


Fig. S2 Thin film Tauc plots of the D–A polymers and PC₇₁BM.

Cyclic Voltammetry (CV)

Cyclic voltammetry (CV) was performed on an ALS/chi-620C electrochemical analyzer. The CV cell consisted of a thin film sample on ITO electrode, a Pt wire counter electrode, and an Ag/AgNO₃ reference electrode. The measurement was carried out using acetonitrile with 0.1 M tetrabutylammonium hexafluorophosphate (Bu₄N⁺PF₆⁻) as a supporting electrolyte. The redox potentials were calibrated with ferrocene as an internal standard.

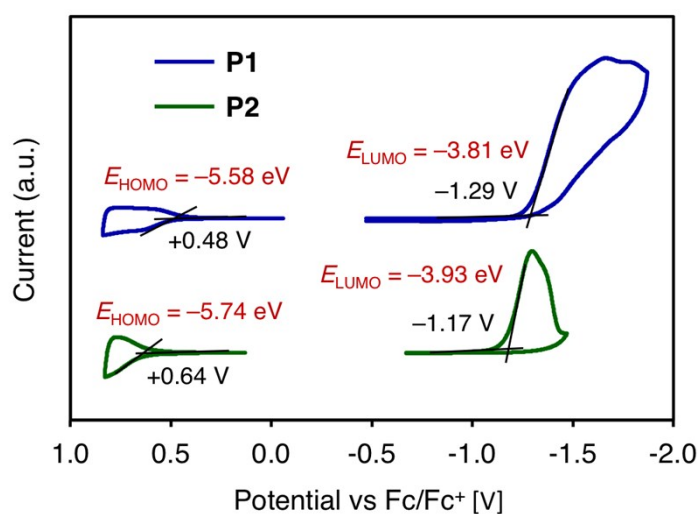


Fig. S3 Cyclic voltammograms of D–A polymers using thin film samples on ITO and 0.1 M ⁿBu₄N⁺PF₆⁻ as a supporting electrolyte. HOMO and LUMO energy level were estimated from the onset potential of the first oxidation and reduction peak ($E_{\text{HOMO}} = -E_{\text{ox,onset}} - 5.1$ eV and $E_{\text{LUMO}} = -E_{\text{red,onset}} - 5.1$ eV), respectively.¹

Theoretical Calculations for the Model Compounds

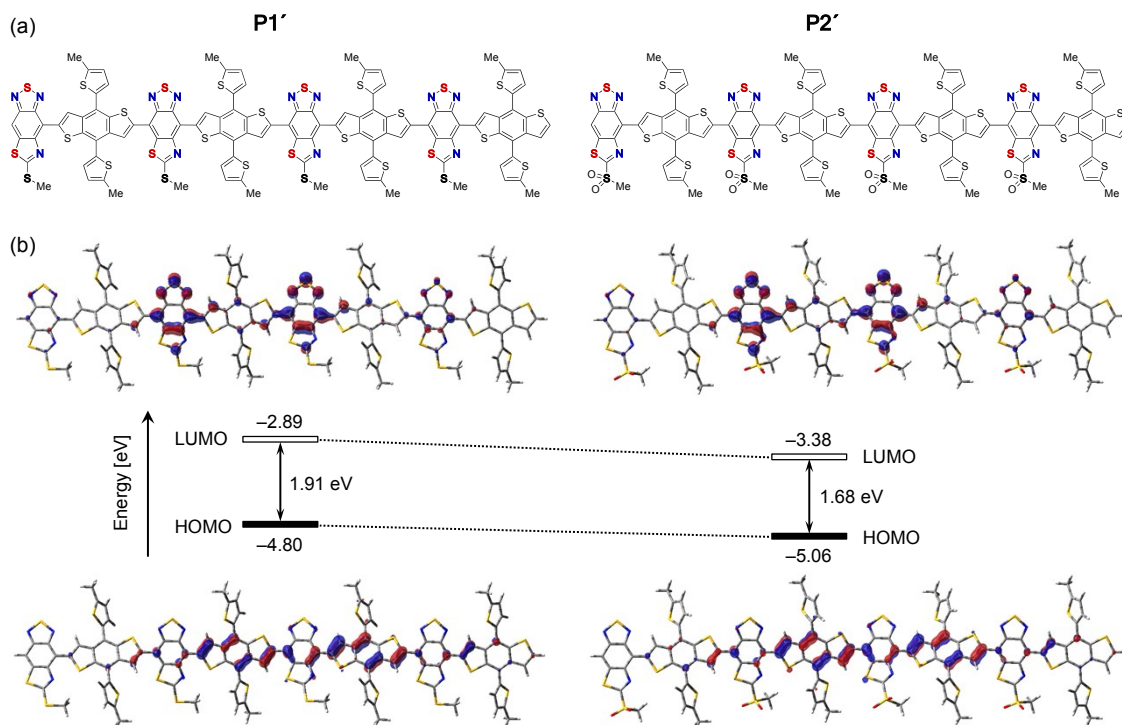


Fig. S4 (a) Chemical structure, and (b) calculated energy diagram and depiction of the frontier orbitals for the tetramer model compounds of the polymers. Calculations were carried out by the DFT method at B3LYP/6-31G(d) level of theory² and the alkyl side chains were replaced with methyl groups to simplify the calculation.

Thin Film Absorption Spectra

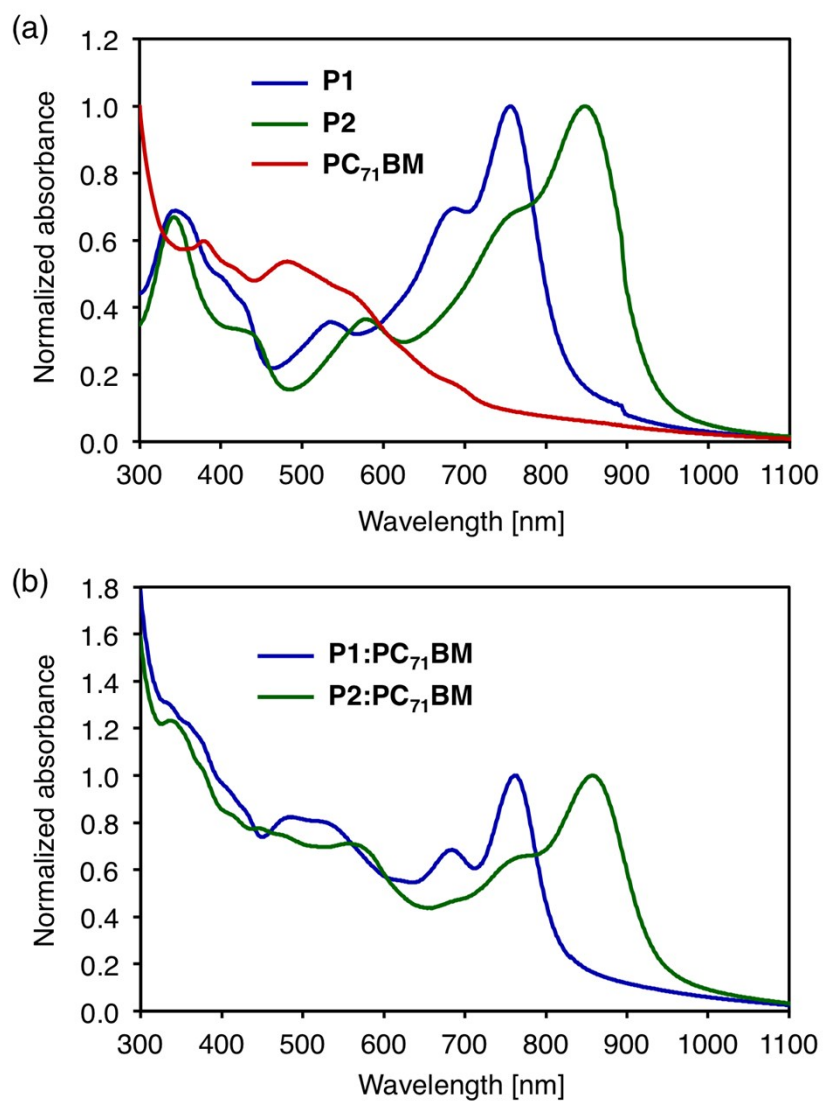


Fig. S5 Thin film absorption spectra of (a) neat films and (b) polymer:PC₇₁BM blends.

Atomic Force Microscopy (AFM)

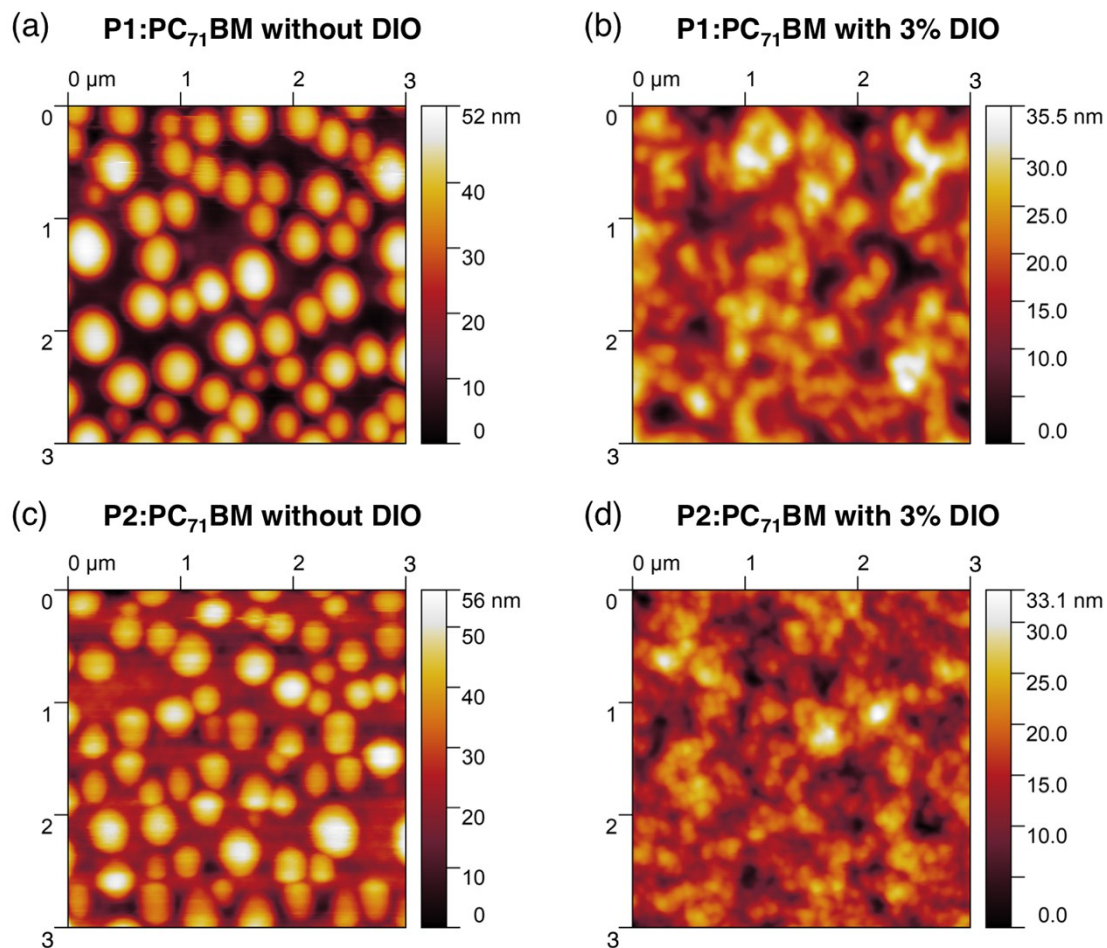


Fig. S6 Surface topographic AFM images of the thin films of **P1:PC₇₁BM** blend on ITO substrates: (a) without DIO and (b) with 3% DIO, **P2:PC₇₁BM** blend (c) without DIO and (d) with 3% DIO.

Photovoltaic Characterization

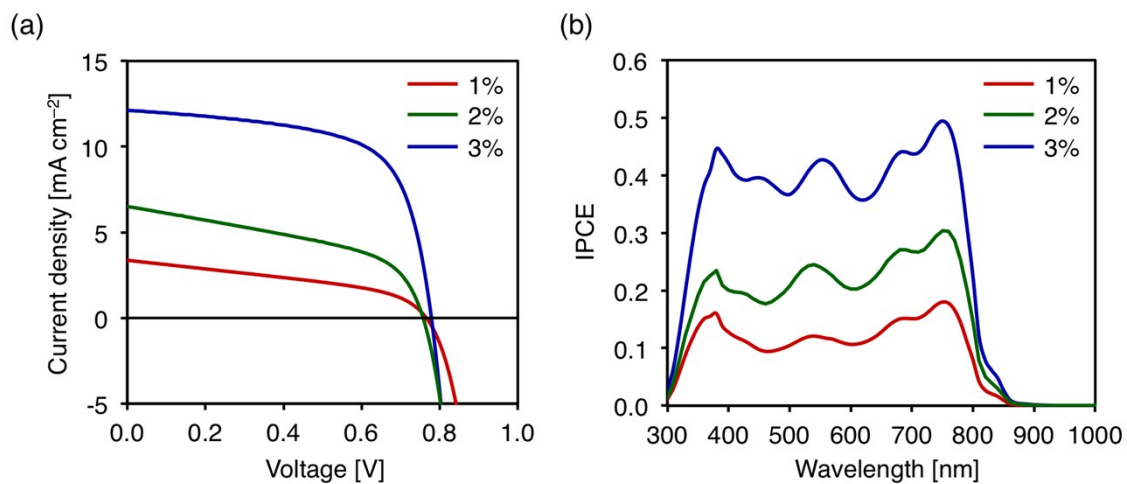


Fig. S7 (a) J - V characteristics and (b) incident photon to current conversion efficiency (IPCE) spectra of **P1**:PC₇₁BM cells. The amount of 1,8-diiodooctane (DIO) is varied from 1 vol% to 3 vol%.

Table S1 Influence of 1,8-Diiodooctane (DIO) Concentration on the Photovoltaic Parameters of **P1**:PC₇₁BM Cells

DIO	J_{SC} [mA cm^{-2}]	V_{OC} [V]	FF	PCE [%]
1 vol%	3.4	0.77	0.41	1.07
2 vol%	6.5	0.76	0.47	2.32
3 vol%	12.1	0.78	0.65	6.13

Space Charge Limited Current (SCLC) Measurements

The hole mobility in the films of materials were measured from the space-charge limited current (SCLC) J - V characteristics obtained in the dark for hole-only devices. Hole mobility was calculated using the Mott-Gurney law by fitting Equation 1, where J is the current density, ϵ_0 is the permittivity of free space (8.85×10^{-12} F m⁻¹), ϵ is the relative permittivity of the material (approaching 3 for organic semiconductors), μ is the hole mobility, V is the applied voltage, and d is the thickness of the active layer, respectively.

$$J = \frac{9}{8} \epsilon \epsilon_0 \mu \frac{V^2}{d^3} \quad (1)$$

The ITO-coated glass substrate ($5 \Omega \text{ cm}^{-2}$, $2.5 \text{ cm} \times 2.5 \text{ cm}$, GEOMATEC) was washed carefully under ultrasonic irradiation using water (15 min), acetone (15 min), detergent solution (Semico Clean 56, Furuuchi chemical) (15 min), water (15 min) and ethanol (15 min). The substrate was further cleaned with a Filgen UV230 UV/ozone cleaner. A thin layer of PEDOT:PSS (Clevious P VP AI 4083) was prepared onto the ITO surface by the spin-coating (5000 rpm, 60 s). The resulting substrate was heated at $140 \text{ }^\circ\text{C}$ for 20 min under ambient conditions. Then, the active layer was deposited by the spin-coating of the chlorobenzene solutions (same for solar cell fabrication) at 600 rpm for 60 s. The film thicknesses were measured with Alphastep IQ (Yamato Scientific Co., Ltd.). As counter electrode, Au was deposited on the film by vacuum evaporation. The current density–voltage curves of the devices were taken with a Keithley 2400 source.

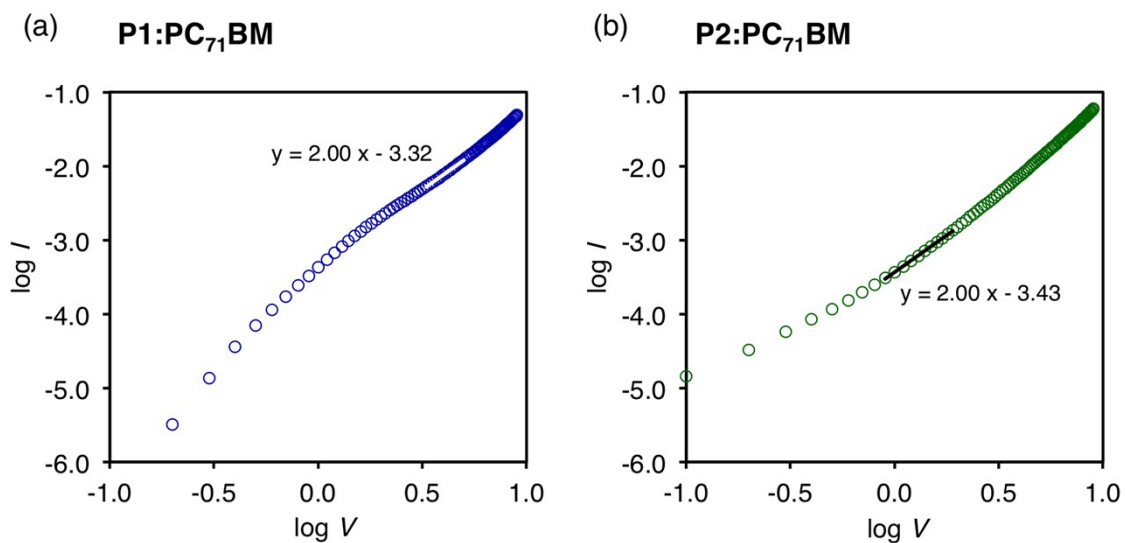


Fig. S8 J - V curves of polymer:PC₇₁BM blend films.

Table S2 Hole Mobility (μ_h) Estimated from J - V Curves of Hole-only Polymer:PC₇₁BM Blend Films

Polymer	Thickness [nm]	μ_h [cm ² V ⁻¹ s ⁻¹] ^a
P1	96	$(1.06 \pm 0.09) \times 10^{-5}$
P2	116	$(1.21 \pm 0.08) \times 10^{-5}$

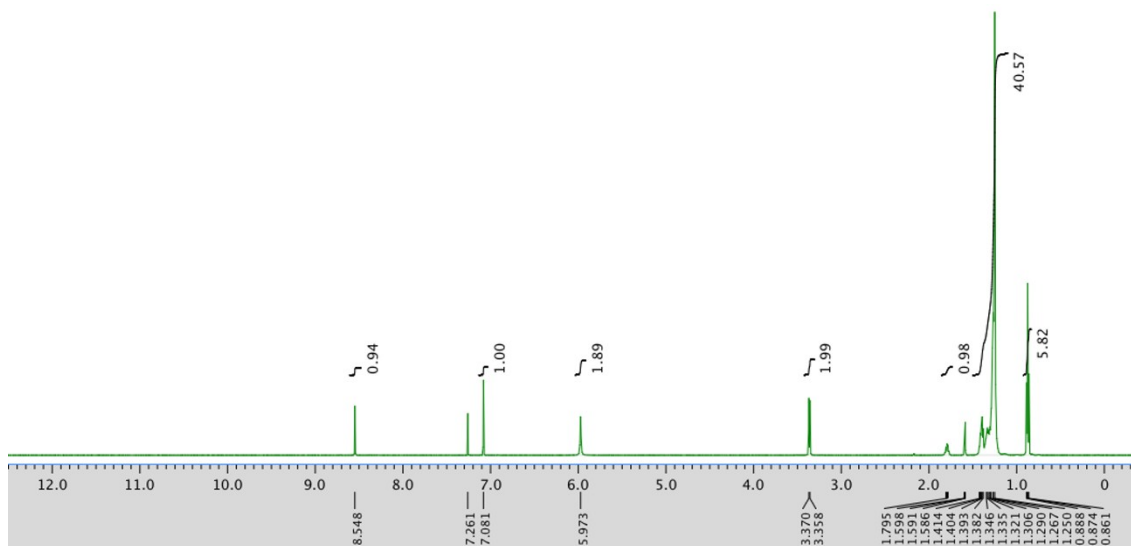
^aAverage hole mobility with standard deviation from 6 samples.

References

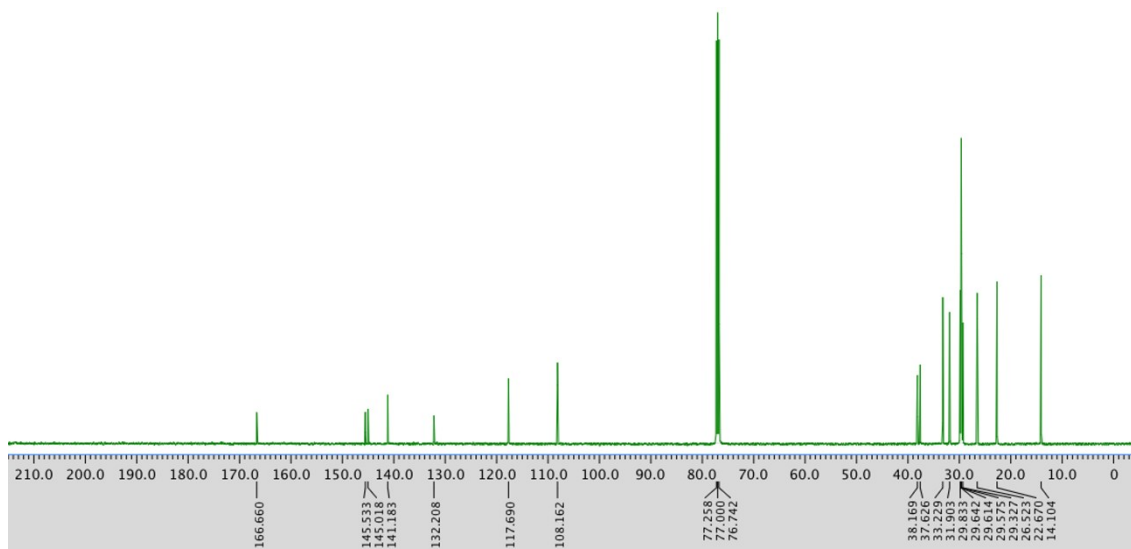
- 1 C. M. Cardona, W. Li, A. E. Kaifer, D. Stockdale, G. C. Bazan, *Adv. Mater.*, 2011, **23**, 2367–2371.
- 2 Gaussian 09, Revision C.01, M. J. Frisch, G. W. Trucks, H. B. Schlegel, G. E. Scuseria, M. A. Robb, J. R. Cheeseman, G. Scalmani, V. Barone, G. A. Petersson, H. Nakatsuji, X. Li, M. Caricato, A. Marenich, J. Bloino, B. G. Janesko, R. Gomperts, B. Mennucci, H. P. Hratchian, J. V. Ortiz, A. F. Izmaylov, J. L. Sonnenberg, D. Williams-Young, F. Ding, F. Lipparini, F. Egidi, J. Goings, B. Peng, A. Petrone, T. Henderson, D. Ranasinghe, V. G. Zakrzewski, J. Gao, N. Rega, G. Zheng, W. Liang, M. Hada, M. Ehara, K. Toyota, R. Fukuda, J. Hasegawa, M. Ishida, T. Nakajima, Y. Honda, O. Kitao, H. Nakai, T. Vreven, K. Throssell, J. A. Montgomery, Jr., J. E. Peralta, F. Ogliaro, M. Bearpark, J. J. Heyd, E. Brothers, K. N. Kudin, V. N. Staroverov, T. Keith, R. Kobayashi, J. Normand, K. Raghavachari, A. Rendell, J. C. Burant, S. S. Iyengar, J. Tomasi, M. Cossi, J. M. Millam, M. Klene, C. Adamo, R. Cammi, J. W. Ochterski, R. L. Martin, K. Morokuma, O. Farkas, J. B. Foresman, and D. J. Fox, Gaussian, Inc., Wallingford CT, 2016.

NMR spectra.

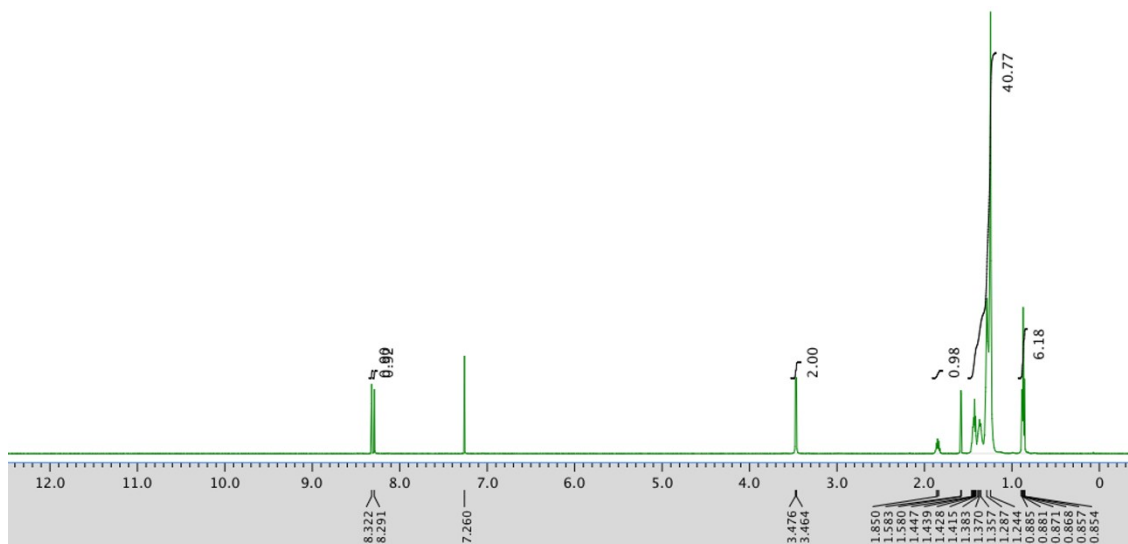
^1H NMR spectrum of **3** (500 MHz, CDCl_3)



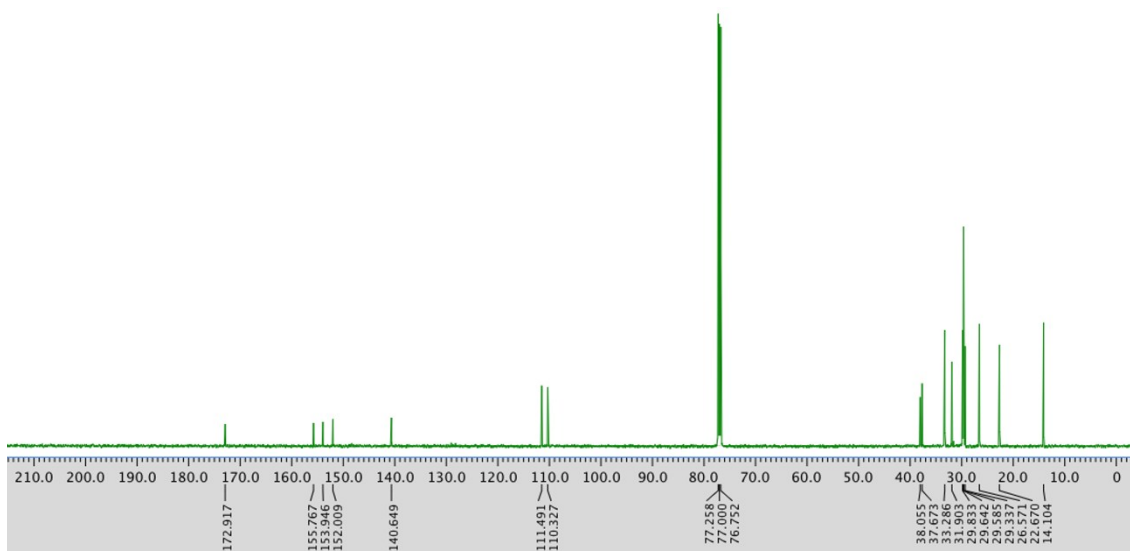
^{13}C NMR spectrum of **3** (126 MHz, CDCl_3)



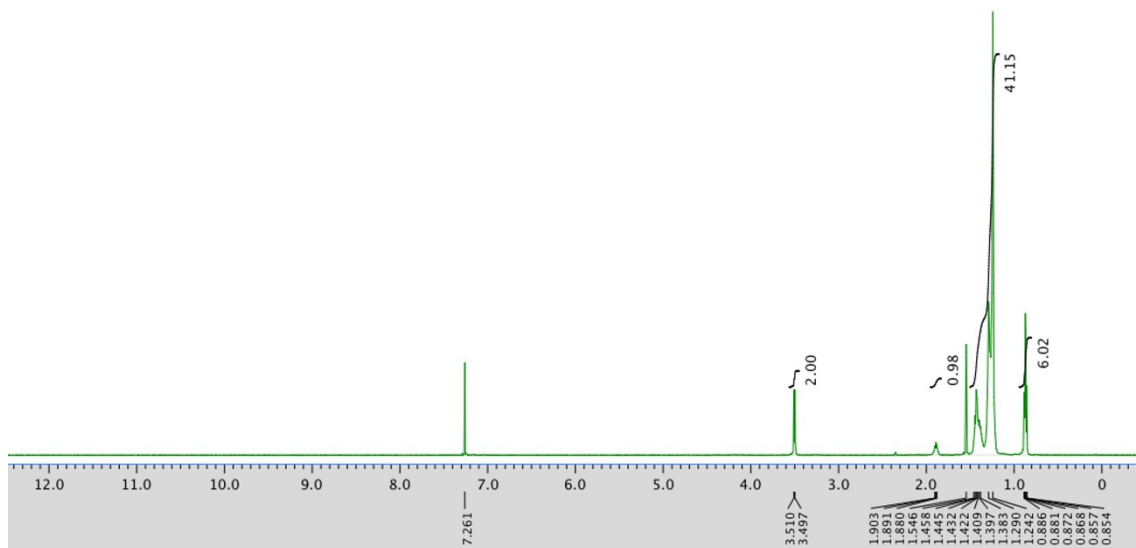
^1H NMR spectrum of **5** (500 MHz, CDCl_3)



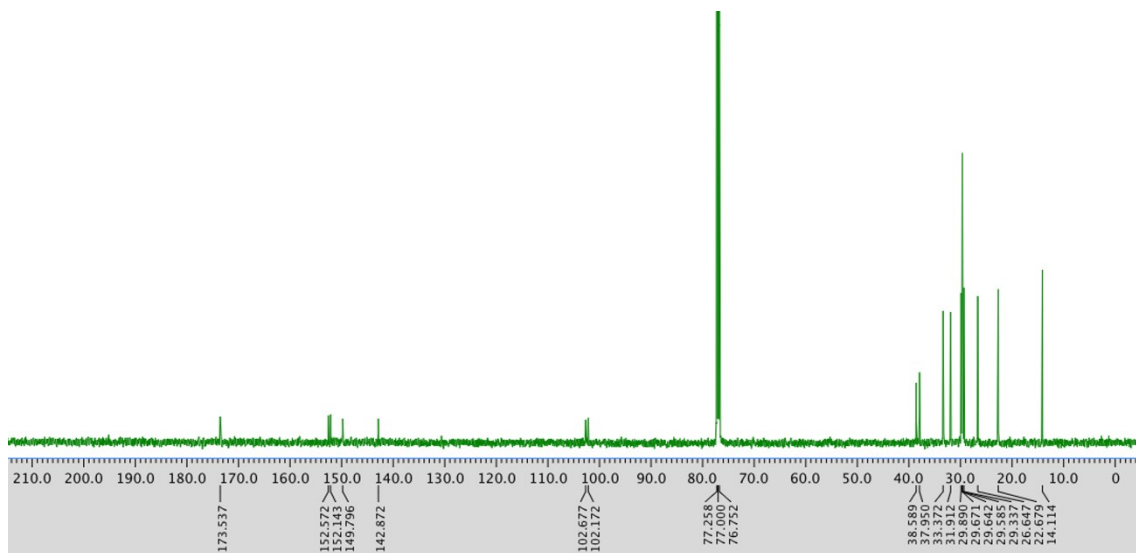
^{13}C NMR spectrum of **5** (126 MHz, CDCl_3)



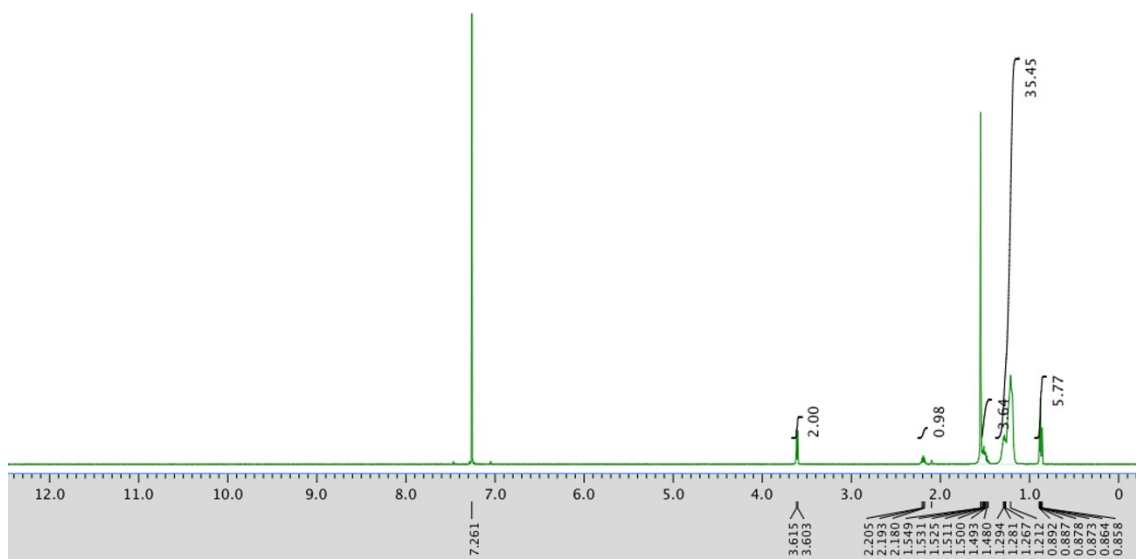
^1H NMR spectrum of **6** (500 MHz, CDCl_3)



^{13}C NMR spectrum of **6** (126 MHz, CDCl_3)



^1H NMR spectrum of **7** (500 MHz, CDCl_3)



^{13}C NMR spectrum of **7** (126 MHz, CDCl_3)

